Available online at www.sciencedirect.com
SCIENCE DIRECT
Talanta 69 (2006) 1176–1181
Talanta
www.elsevier.com/locate/talanta

Extending the dynamic range of copper determination in differential pulse adsorption cathodic stripping voltammetry using wavelet neural network

T. Khayamian, Ali A. Ensafi *, A. Benvidi

College of Chemistry, Isfahan University of Technology, Isfahan 84156, Iran

Received 7 August 2005; received in revised form 12 December 2005; accepted 15 December 2005
Available online 19 January 2006

Abstract

A wavelet neural network (WNN) model is proposed for extending the dynamic range of Cu(II) determination by differential pulse adsorption cathodic stripping voltammetry (DP-AdSV) using xylenol orange (XO) as a suitable ligand. All of voltammograms data consisting of Cu(II) and Cu(II)–XO peak currents were used in WNN model. The WNN model consisted of three layers (2-8-1) with the Morlet mother wavelet transfer function in the hidden layer. The model was able to extend the dynamic range of Cu(II) from its narrow linear range (1–50 ng ml^{-1}) to the higher dynamic range (1–1500 ng ml^{-1}). The results of the WNN model was also compared with artificial neural network (ANN) model and it was demonstrated the superiority of the WNN model relative to ANN model.

Keywords: Copper; Extending dynamic range; Xylenol orange; Voltammetry; Wavelet

1. Introduction

Copper is an element, which is used widespread in industries such as metallurgy, electronics, heating, etc. In addition, copper is a metal of prime environmental concern. Voltammetric techniques are suitable techniques for the determination of trace elements in aquatic system, such as river, lakes, and sediments owing to their sensitivity, simplicity and simple sample pretreatment [1]. Several electrochemical stripping procedures including anodic stripping voltammetry (ASV) and adsorptive cathodic stripping voltammetry (AdCSV) have been reported for the determination of copper [2–6]. The disadvantages of the anodic stripping voltammetry method have been reviewed [4,7]. In order to eliminate the limitations of anodic stripping voltammetry for copper determination, an organic ligand is used to complex with copper(II) with adsorptive property rather than an electrolytic accumulation on the electrode surface. Several papers have been reported and compared [4,7] using of adsorptive cathodic stripping voltammetry for the determination of copper. The main limitation of adsorptive methods for determination of Cu(II) was low dynamic range. Artificial neural network (ANN) can model non-linear systems and therefore, they can be used in analytical chemistry for non-linear calibration curves modeling [8–12]. ANN was used for extending the response range of an optical fiber pH sensor [13]. It was also used for extending the dynamic range of the determination of copper by AdCSV [14]. However, according to our knowledge, this is the first report for extending the dynamic range of an electro-analytical method using wavelet neural network (WNN). The WNN has been proposed as a novel universal tool for functional approximation, which shows surprising effectiveness in solving the conventional problem of poor convergence or even divergence encountered in other kind of neural networks. It can dramatically increase convergence speed. In spite of the WNN having great potential applicability, there are only a few papers on WNN and its application to chemistry [15–17]. Guo and co-workers [15] have WNN for prediction of driving forces of α-cyclodextrin complexation with benzene derivatives and the inclusion of β-cyclodextrin with benzene derivatives. Liu and co-workers [8] have been used WNN for prediction of programmed temperature retention values of naphtas. Recently we have been used WNN for prediction of critical micelle concentration

* Corresponding author. Tel.: +98 311 3912351; fax: +98 311 3912350.
E-mail address: Ensafi@cc.iut.ac.ir (A.A. Ensafi).

0039-9140/$ – see front matter © 2005 Elsevier B.V. All rights reserved.
doi:10.1016/j.talanta.2005.12.033

of Gemini surfactants [16] and prediction of solubility for some polycyclic aromatic hydrocarbons in supercritical CO_2 [17].

The same as ANN, WNN consists of three layers: input layer, hidden layer and output layer. WNN have been proposed based on the theories of feed-forward neural networks and wavelet decomposition. The network learns by calculating an error between desired and actual outputs and propagating this error back to each node. The output value of the sample V_n is calculated with the following formula [8,15]:

$$V_n = \sum_{t=1}^{T} W_t f\left(\frac{\sum_{i=1}^{s} w_{ti} x_n(i) - b_t}{a_t}\right) \quad (1)$$

where f is taken as a Morlet mother wavelet:

$$f(t) = \cos(1.75t)\exp\left(-\frac{t^2}{2}\right) \quad (2)$$

In these equations, $x_n(i)$ represents the input data and V_n represents the corresponding output value, where i varies from 1 to s. w_{ti} and W_t represent weights, a_t and b_t are dilation and translation parameter, respectively. The number of nodes, n, represents the nth data sample of training set, and T represents the target output state. To reduce the error, W_t, w_{ti}, a_t, b_t are adjusted based on gradient descend algorithm [8,15].

A wavelet neural network model is proposed for extending the dynamic range of Cu(II) determination by differential pulse adsorption cathodic stripping voltammetry (DP-AdSV) using xylenol orange as a suitable ligand. In this work, instead of using currents of voltammogram in different voltages, the scores of the principal components analysis (PCA) of the response data were used as input values for neurons in the input layer. This dimensionality reduction step by PCA before non-linear WNN model construction, increases the numerical stability of the model construction process and reduces the amount of co-linearity between variables.

2. Experiment

2.1. Apparatus

A Princeton Applied Research (PAR, EG&G) Model 384B polarographic analyzer system, with a PAR 303A static mercury drop electrode and an Ag/AgCl reference electrode, a PAR Model 305 stirrer that link with a computer (Pentium III) with Sigma Plot software and a Model DMP 40–44 plotter were used. A conventional three electrode system, comprising a small-sized hanging mercury drop electrode (HMDE), with a surface area of 1.6 mm^2, a platinum wire counter electrode and an Ag/AgCl (in saturated with KCl) reference electrode were used in all experiments. All potentials reported were referred to the Ag/AgCl electrode. Solutions were deoxygenated with high-purity nitrogen for 4 min prior to each experiment and it was performed under a nitrogen atmosphere.

2.2. Reagents

All reagents used were analytical reagent-grade and double distilled water was used throughout.

A xylenol orange (XO) solution, 1.0×10^{-4} M, was prepared by dissolving appropriate amount of the compound (Merck) in distilled water.

A stock solution of Cu(II), 1000 mg L^{-1}, was prepared by dissolving appropriate amount of copper nitrate (Merck) in distilled water.

Buffer solution was prepared from acetate buffer (0.5 M).

2.3. Recommended procedure

The supporting electrolyte solution (10 ml of 0.02 M acetate buffer solution, pH 5.0) containing 4.0×10^{-6} M xylenol orange was pipetted into the cell and purged with nitrogen gas for at least 4 min. An adsorption potential, −0.60 V versus Ag/AgCl, was applied to a fresh hanging mercury drop electrode in quiescent solution, and adsorption was carried out from the stirred solution for a period of 90 s, then a differential pulse cathodic stripping voltammogram was recorded from +0.20 to −0.15 V with a potential scan rate of 10 mV s^{-1} and a pulse amplitude of 80 mV. After the background voltammogram was obtained, the copper(II) standard solution was introduced into the cell while maintaining a nitrogen atmosphere over the solution and a differential pulse cathodic stripping voltammogram was recorded as described above to give the sample peak current. At last at the supposed voltage range (+0.20 to −0.15 V) with scan rate of 10 mV s^{-1}, the current of 176 points of the voltage were measured. All data was obtained at room temperature.

2.4. Hardware and software environment

Data processing was performed by a Pentium III computer. The algorithm was written in MATLAB (Math Work, version 6.1) by the authors.

3. Results and discussions

Preliminary experiments were carried out to identify the general features, which characterize the behavior of the Cu(II)–xylenol orange system on a HMDE. xylenol orange can form a complex with Zn(II), Pb(II) and Cu(II) at different pH values. Copper(II) can make a 1:1 complex with XO [18,19]. The formation constant of complex of Cu(II)–xylenol orange is log $K_f = 7.2$ at pH range of 5–7 [18,19].

Fig. 1 shows the stripping voltammograms of the ligand–buffer, Cu(II)–buffer and Cu(II)–ligand–buffer system at pH 5.0 and in the potential range of +0.20 to −0.15 V versus Ag/AgCl reference electrode. According to Fig. 1a and b, no obvious current are observed in this potential range, for the ligand–buffer and Cu(II)–buffer system. With the addition of xylenol orange to Cu(II)–buffer system, as indicated in Fig. 1c, a large cathodic peak current located at about 0.00 V was obtained. Addition of 10 μg ml^{-1} Triton X-100 cause reducing the peak current to about 10% of the initial value. In addition, in linear

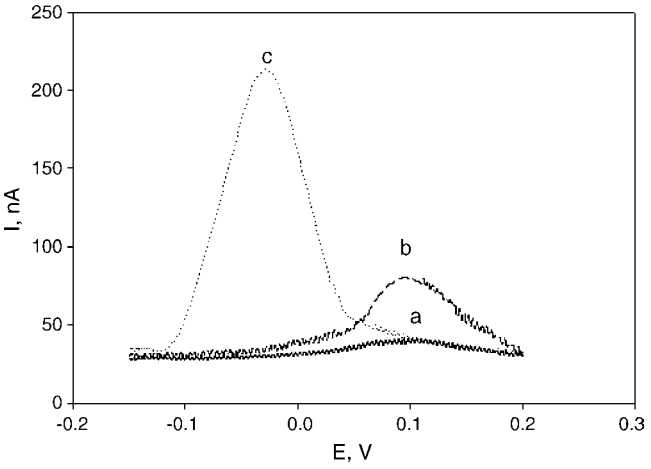

Fig. 1. Differential pulse cathodic stripping voltammograms of (a) blank solution; (b) Cu(II) solution without the ligand; (c) Cu(II) solution in the presence of xylenol orange.

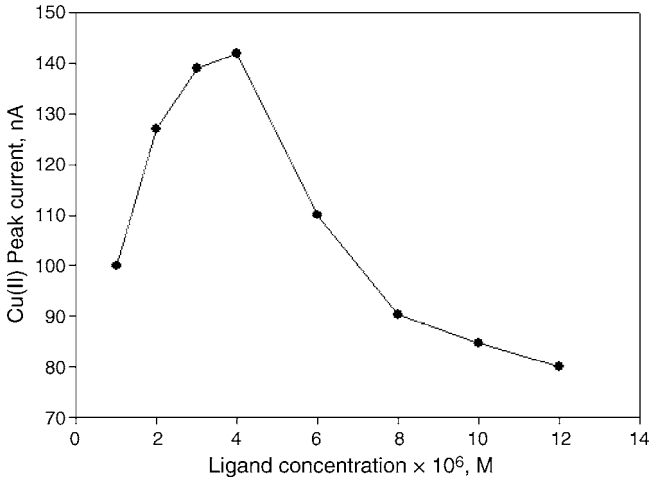

Fig. 3. Influence of xylenol orange concentration on the peak current.

sweep voltammetry, Cu(II)–XO peak currents versus scan rate (between 20 to 100 mV s^{-1}) showed a linear relationship (Fig. 2). These phenomena show the adsorptive characteristic of the complex.

Under the optimized conditions, a calibration graph was obtained from 1.0 to 50.0 ng ml^{-1} for the Cu(II)–XO system. The main problem of the Cu(II)–XO system for determination of copper is the low dynamic range of determination. In this paper, we have tried to extend the dynamic range of copper determination by using WNN and ANN model.

3.1. Effect of variables

The pH dependence of the adsorption peak current of 30 ng ml^{-1} Cu(II) solution was studied with xylenol concentration of 3.0×10^{-6} M, scan rate of 10 mV s^{-1}, pulse height of 80 mV, accumulation potential of −0.50 V and accumulation time of 90 s. The results showed that by increasing pH value from 1.5 to 2.0, the peak current increased whereas, higher pH values decreased the peak current. However, as Cu(II) and Cu(II)–XO have separated peak at pH 5.0, a pH of 5.0 was selected for further study.

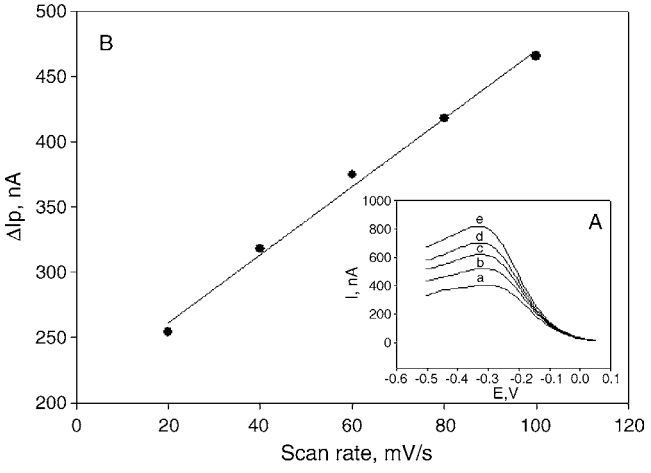

Fig. 2. (A) Linear sweep voltammograms of Cu(II)–XO in different scan rates: (a) 20; (b) 40; (c) 60; (d) 80; (e) 100 mV s^{-1}. (B) Dependence of peak current on the scan rate. Conditions: pH 5.0; Cu(II) concentration 1.0×10^{-4} M; XO concentration 5.0×10^{-4} M.

Since the presence of XO as a ligand is essential for formation of the adsorptive complex, the influence of XO concentration on the peak current was studied. Variation of peak current with XO concentration showed that the peak current increased by increasing of XO concentration up to 4.0×10^{-6} M, whereas a decrease in the peak current of Cu(II)–XO was observed for higher XO concentrations value (Fig. 3). This is due to the competition of XO with Cu(II)–XO for adsorption on the HMDE. Therefore, an optimum XO concentration of 4.0×10^{-6} M was selected for further study.

The influence of pulse height on the peaks current of Cu(II)–XO also studied with pH of 5.0, accumulation potential of −0.60 V, accumulation time of 90 s, XO concentration of 4.0×10^{-6} M, and Cu(II) concentration of 40 ng ml^{-1}. The results showed that increasing in pulse height from 20 to 100 mV increased the peak current, whereas higher pulse height (>80 mV) caused peak broadening. Therefore, a pulse height of 80 mV was selected which presented appropriate shape of the peak. In addition, the influence of scan rate on the peak current of Cu(II)–XO was also studied with the above optimum conditions. The results showed that with scan rate of 10 mV s^{-1}, the peak current was at maximum value. Therefore, a scan rate of 10 mV s^{-1} was selected.

The influence of accumulation potential on the peak current of Cu(II)–XO was studied over the range of 0.00 to −1.00 V. The results showed that the peak current increases and gets maximum when the accumulation potential changed from 0.00 to −0.60 V, whereas more negative potential values caused decreasing the peak current. Therefore, −0.60 V was selected as a suitable accumulation potential for the study.

The influence of accumulation time on the peak current of Cu(II)–XO was studied in the range of 0.0–180 s, under the optimized conditions introduced above. The results showed that by increasing accumulation time up to 90 s the peak current increased, then it's leveled off. Therefore, as a compromise

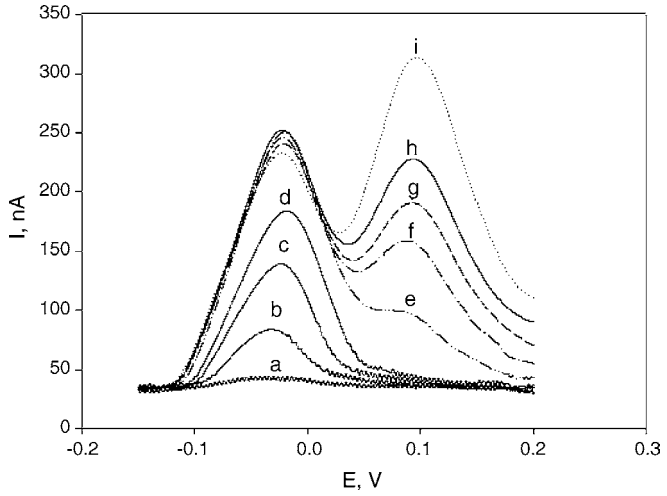

Fig. 4. Differential pulse adsorption cathodic stripping voltammograms of Cu(II) solutions under the optimized conditions: (a) blank; (b) 10 ng ml^{-1}; (c) 25 ng ml^{-1}; (d) 40 ng ml^{-1}; (e) 125; (f) 210 ng ml^{-1}; (g) 250 ng ml^{-1}; (h) 350 ng ml^{-1}; and (i) 450 ng ml^{-1} Cu(II).

between sensitivity and time of analysis, an accumulation time of 90 s was selected for further study.

The differential pulse stripping voltammograms for different concentration of Cu(II) under the optimized conditions are shown in Fig. 4 for Cu(II)–XO system by DP-AdCSV. As shown in this figure, when trace amount of Cu(II) was added to the blank solution containing XO, a cathodic peak current located at approximately 0.00 V was obtained that related to Cu(II)–XO complex. On the other hand, when higher amounts of copper(II) added to the blank solution, a second cathodic peak current located at approximately +0.10 V was obtained that was related to free Cu(II) ions. In addition, with increasing XO concentration, the first peak decreased and the second peak increased.

According to the above results, we can guess that for the first step, XO make a complex with Cu(II):

$$\mathrm{Cu(II)} + \mathrm{XO} \rightarrow \mathrm{Cu(XO)} \quad (3)$$

As described above, the results for study of accumulation potential on the peak current showed that the optimum accumulation potential (−0.60 V) is more negative than the Cu(II)–XO reduction peak. Therefore, we think that during accumulation time of 90 s, the complex was accumulate at the surface of HMDE and then reduces as:

$$\mathrm{Cu(XO)} + 2\mathrm{e} \rightarrow \mathrm{Cu(s)} + \mathrm{XO} \quad (4)$$

Differential pulse voltammograms of a solution containing 500 ng ml^{-1} Cu(II) and 4×10^{-6} M of XO without accumulation and with 90 s accumulation show two peaks. Without accumulation, both peak currents were shorter than those peak currents with accumulation time of 90 s. It shows that at potential of −0.60 V, Cu(II) and Cu(II)–XO reduce to Cu and accumulate. After jumping of potential from −0.60 to +0.20 V, copper oxidizes to Cu(II) and make a complex with XO around the HMDE. With high concentration of Cu(II) in the solution, as described before, the excess of free Cu(II) remains at the surface of the electrode. Therefore, we have two different reduction peaks, first is due to the uncomplexed Cu(II) (free ions at +0.10 V) and the second is due to Cu(II)–XO complex (at 0.00 V).

Under the above conditions, Cu(II)–XO peak current is proportional to the concentration of Cu(II) in the range of 1–50 ng ml^{-1} of Cu(II). As we said previously, the main problem of the Cu(II)–XO complex system for the determination of copper is the short dynamic range. Therefore, WNN was used to extend the dynamic range of the method.

3.2. Wavelet neural network method

Forty standard solutions were prepared with different copper concentration from 1.0 to 1500 ng ml^{-1}. The 26 standard solutions were randomly chosen for the training set and 14 solutions were selected for the prediction set. The differential pulse voltammogram was recorded from +0.20 to −0.15 V for each sample. Therefore, the response data of the training set was a matrix with 26 × 176 dimensions.

At first, the data matrix of the training set was analyzed by principal component analysis. The result of this data was 11 PCs. The scores of the PCs were chosen as input nodes for the input layer. The number of PC and the number of neurons in the hidden layer are unknown and need to be optimized. In addition, the WNN parameters consist of the learning rate, the momentum and the number of iterations should be optimized. In this work, the numbers of PC, number of neurons in the hidden layer and other parameters except the number of iterations were optimized simultaneously. The procedure was conducted by the following way. A MATLAB program was written to change the number of PCs from 1 to 11, and the number of neurons in the hidden layer from 2 to 12, while the learning rate was changed from 0.002 to 0.2 with a step of 0.002 and the momentum was changed from 0.02 to 0.9 with a step of 0.02. The root mean square errors (RMSEs) for the calibration and prediction sets were calculated for all of the possible combinations of values for the mentioned

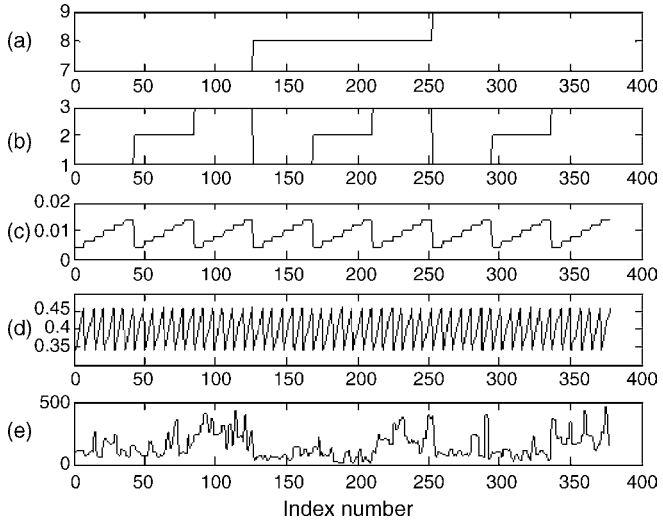

Fig. 5. Plots of (a) the number of neurons in the hidden layer against the index number; (b) the number of PCs used in the input layer against the index number; (c) the learning rate against the index number; (d) the momentum against the index number; and (e) the RMSE for the prediction set against the index number.

Table 1
Experimental and calculated values of Cu(II) concentrations using ANN and WNN models for the prediction set

Absolute error (WNN)	Cal. (WNN)	Absolute error (ANN)	Cal. (ANN)	Exp.
0.2	3.2	0.2	3.2	3.0
−0.3	5.7	−0.4	5.6	6.0
3.5	23.5	3.5	23.5	20.0
−6.3	28.7	−3.4	31.6	35.0
−2.9	57.1	1.0	61.0	60.0
−8.4	81.6	−12.7	77.3	90.0
25.6	205.6	19.5	199.5	180.0
8.5	308.5	51.0	351.0	300.0
−3.8	456.2	−42.5	417.5	460.0
31.9	681.9	52.2	702.2	650.0
−49.0	648.1	73.3	773.3	700.0
23.0	1023.7	59.3	1059.3	1000.0
−20.0	1320.0	−11.0	1329.0	1340.0
72.6	1572.6	80.9	1580.9	1500.0

variables. Fig. 5 shows the changes of the variable values versus index number. Each number of index number corresponds to a combination of variable values and total number of index numbers is equal to the possible combinations for variable values. The subset of index numbers is shown in Fig. 5. The RMSE for prediction set for each number of index number is calculated and the RMSE versus a subset of the index number is also shown in Fig. 5e. It was realized that the RMSE errors for the prediction set was minimum, when two PCs and eight neurons were selected for input and hidden layers, respectively. While the learning rate and momentum values were 0.01 and 0.40, respectively. Finally, the number of iterations was optimized with the optimum values for the variables. The RMSE for the prediction set was minimum at 3050 numbers of iterations. The performance of the model was evaluated by plotting the predicted Cu(II) concentration by the model versus the copper concentration in standard solutions of the prediction set. The result is given in Table 1 and is shown in Fig. 6. In addition, the absolute error values were calculated for the prediction set using ANN and WNN models are given in Table 1. The average relative error for prediction set is 7.3%.

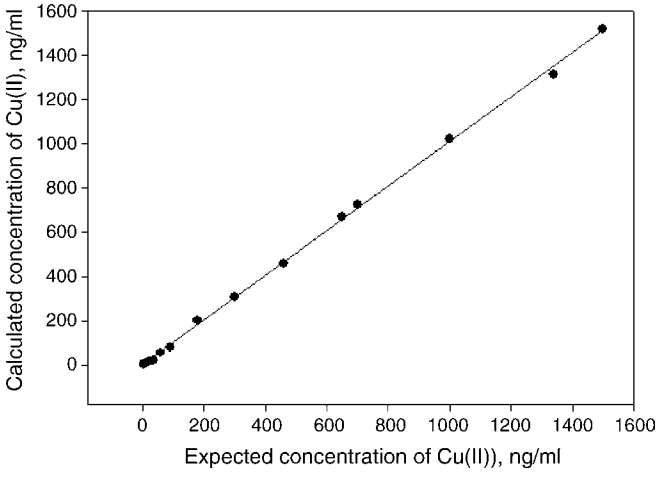

Fig. 6. Relation between expected concentration of Cu(II) and calculated concentration of Cu(II) was determined by WNN (2-8-1).

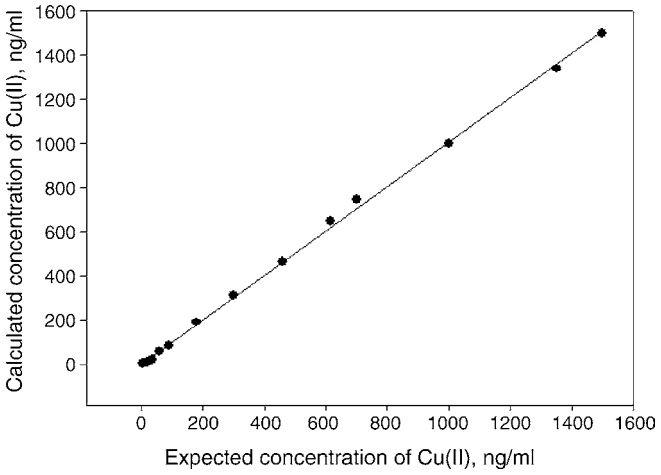

Fig. 7. Relation between expected concentration of Cu(II) and calculated concentration of Cu(II) was determined by ANN (3-10-1).

Therefore, small error of prediction set indicates good performance of the model.

3.3. Artificial neural network method

In order to compare the predictive ability with another nonlinear model, a similar study was carried out using ANN model. A neural network was constructed with a sigmoid function as the hidden transfer function and a linear function as the output transfer function. A back propagation learning algorithm was employed to adjust the weights. The ANN architecture and its parameters were optimized simultaneously as the same as WNN. It was realized that RMSE for the training and prediction sets are minimum when two PCs and one bias in the input layer and 10 neurons were selected in the hidden layers and when the learning rate and the momentum values were 0.11 and 0.18, respectively. The RMSE for prediction set was minimum after 10,200 iterations. The performance of the model was also evaluated by plotting the ANN calculative concentrations of Cu(II) versus experimental concentration of Cu(II) (Fig. 7). The average relative error for prediction set is 9.0%.

According to the obtained results, in compare with ANN, WNN converges faster and has higher accuracy. So WNN is a more powerful tool for dealing with nonlinear model compared with the ANN.

4. Conclusion

The ANN and WNN model were used for extending the dynamic range of Cu(II) with adsorption differential pulse stripping voltammetry method. The ANN and WNN architecture including the number of PCs as input layer and the number of neurons in the hidden layer as well as other parameters were optimized simultaneously. The ANN and WNN model are able to extend the dynamic range about 1.8 orders of magnitude. The comparison of results obtained from two different methods shows that the WNN has slightly better accuracy and faster convergence.

Acknowledgements

The authors are thankful to the Isfahan University of Technology Research Council and Center of Excellence in Sensor (IUT) for the support of this work.

References

[1] K. Stulik, R. Kalvoda, Electrochemistry for Environmental Protection, Charle University and Academy of Science of the Czech Republic, 1995.
[2] W.W. Kubiak, R.M. Latonen, A. Ivaska, Talanta 75 (2001) 119.
[3] L. Jin, N.J. Gogan, Anal. Chim. Acta 412 (2000) 77.
[4] R. Hajian, E. Shams, Anal. Chim. Acta 491 (2003) 63.
[5] O.A. Farghali, Microchem. J. 75 (2003) 119.
[6] A.A. Ensafi, S. Abbasi, H. Rahimi Mansour, I. Mohammad pour, Anal. Sci. 17 (2001) 609.
[7] A.A. Ensafi, M. Atabati, Anal. Lett. 33 (2000) 1591.
[8] X. Zhang, J. Qi, R. Zhang, M. Liu, Z. Hu, H. Xue, B. Fan, Comp. Chem. 25 (2001) 125.
[9] W. Guo, P. Zhu, H. Brodowsky, Talanta 44 (1997) 1995.
[10] A.A. Ensafi, T. Khayamian, M. Atabati, Talanta 57 (2002) 785.
[11] M.H. Fatemi, J. Chromatogr. A 955 (2002) 273–280.
[12] H. Chan, A. Butler, D.M. Falck, M.S. Freund, Anal. Chem. 69 (1997) 2373.
[13] M.N. Taib, R. Andres, R. Narayanaswamy, Anal. Chim. Acta 330 (1996) 31.
[14] T. Khayamian, A.A. Ensafi, M. Atabati, Microchem. J. 65 (2000) 347.
[15] L. Liu, Q. Guo, J. Chem. Inf. Sci. 39 (1999) 133.
[16] Z. Kardanpour, B. Hemmateenejad, T. Khayamian, Anal. Chim. Acta 531 (2005) 285.
[17] T. Khayamian, M. Esteki, J. Supercrit. Fluids 32 (2004) 73.
[18] J. Lurie, Handbook of Analytical Chemistry, Mir Publisher, 1978, p. 250.
[19] K. Ogura, K. Seneo, S. Muracami, T. Yosino, J. Inorg. Nucl. Chem. 42 (1980) 1165.